JACS
JOURNAL OF THE AMERICAN CHEMICAL SOCIETY
Article
pubs.acs.org/JACS

Unraveling the Pathway of Gold(I)-Catalyzed Olefin Hydrogenation: An Ionic Mechanism

Aleix Comas-Vives*[,†,‡] and Gregori Ujaque*[,‡]

[†]Department of Chemistry, ETH Zürich, Wolfgang-Pauli-Strasse 10, CH-8093 Zürich, Switzerland

[‡]Unitat de Química Física, Departament de Química, Edifici Cn, Universitat Autònoma de Barcelona, E-08193 Bellaterra, Catalonia, Spain

Supporting Information

ABSTRACT: The reaction mechanism of olefin hydrogenation catalyzed by the bimetallic gold catalyst {$(AuCl)_2$[(*R*,*R*)-Me-DuPhos]} was studied by means of density functional theory calculations. This catalyst is enantioselective for the homogeneous hydrogenation of olefins and imines. The reaction mechanism involves activation of the H_2 molecule. This process takes place heterolytically, generating a metal−hydride complex as the active species and releasing a proton (formally $EtOH_2^+$) and a chloride ion to the medium. The hydrogenation reaction proceeds through an ionic mechanism in which the gold catalyst provides a hydride and the proton comes from the solvent. The reaction mechanism ends up with H_2 coordination and subsequent heterolytic cleavage, regenerating the gold(I)−hydride active species. Significant differences were found in the reaction mechanism depending on the nature of the substrate (ethene, cyclohexene, or diethyl 2-benzylidenesuccinate) and the character of the catalyst (mono- or bimetallic). Our data suggest that for prochiral substrates, the step that determines the enantioselectivity within the ionic mechanism involves a proton transfer.

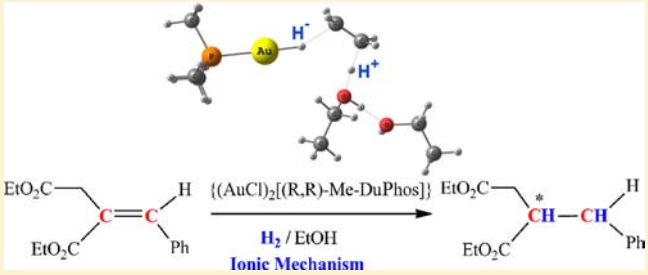

1. INTRODUCTION

Gold-based catalysts have been found to be active in several homogeneous and heterogeneous reactions of organic substrates, such as oxidations and nucleophilic additions to alkenes, allenes, and alkynes as well as hydrogenations.[1] In several cases, the performance of gold catalysts even surpasses that of other common transition-metal catalysts. In this so-called golden era, asymmetric catalysis with gold has not grown so rapidly.

The first case reported dates from more than 20 years ago, when Ito and co-workers found that the addition of an isocyanoacetate to an aldehyde produces the corresponding trans isomer with an enantiomeric excess (ee) of 96%. In that case, cationic gold in combination with a chiral diphosphanylferrocene ligand was used as the catalyst.[2]

In fact, there are few examples of gold-catalyzed asymmetric reactions,[3] and it is one of the challenges of this novel chemistry. In 2005, the first gold catalyst able to perform enantioselective hydrogenation, having the formula {$(AuCl)_2$[(*R*,*R*)-Me-DuPhos]} [Me-DuPhos = 1,2-bis(2,5-dimethylphospholanyl)benzene] was reported by Corma and co-workers.[3b] This catalyst is able to catalyze the asymmetric hydrogenation of olefins and imines, reaching activities comparable to those reported for analogous Pt and Ir complexes but with higher ee values (Scheme 1).[3b] Nevertheless, neither the reaction mechanism nor the origin of the enantioselectivity is yet understood. Hence, further mechanistic insights are needed to improve the overall understanding of these hydrogenation processes.

Scheme 1. The Hydrogenation Reaction Studied in This Work

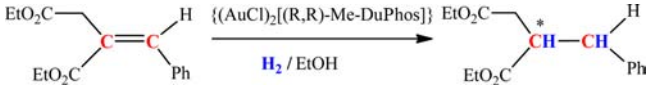

The reaction mechanisms for hydrogenation processes can be classified in inner-sphere and outer-sphere mechanisms according to the interaction between the substrate and the catalyst.[4] The former involves coordination of the double bond to the metal center, whereas the latter does not. The concept of a metal−ligand bifunctional catalyst developed by Noyori is a paradigmatic example of the outer-sphere mechanism.[5] This mechanism has been found to be operative in many other metal−ligand bifunctional catalysts, as shown by Morris and co-workers[6] and others,[7] and even directly in hydrogen transfer by means of ammonia borane.[8] These mechanisms have generally been proposed for hydrogen-transfer reactions to polar double bonds, although the hydrogenations of nonpolar double and triple bonds have been also described.[9]

Eisenstein, Crabtree, and co-workers recently reported a new outer-sphere pathway in which the reaction takes place via a proton transfer and a hydride transfer in two separate steps.[10] Despite the array of inner- and outer-sphere hydrogenation

Received: June 11, 2012
Published: December 5, 2012

dx.doi.org/10.1021/ja305630z | *J. Am. Chem. Soc.* 2013, 135, 1295−1305

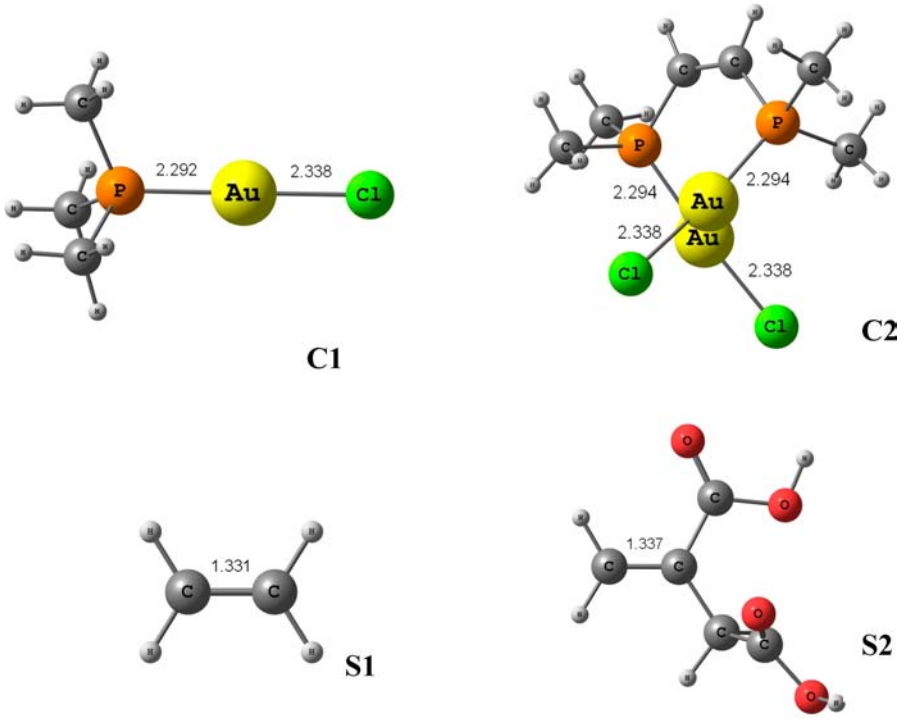

Figure 1. Structures of the catalyst and substrate models used in the calculations. Distances in Å are shown.

mechanisms, no proposals have been found for the case of Au(I)-catalyzed hydrogenation. The present catalyst has neither a ligand suitable for metal−ligand bifunctional catalysis nor the ability to accommodate the hydrides and the alkene for insertion through an inner-sphere mechanism.

The application of theoretical methods to mechanistic analysis of homogeneous catalysis is very helpful,[11] and gold catalysis is not an exception.[3d,12] Paradoxically, the mechanisms of hydrogenation reactions employing homogeneous gold catalysts have remained mostly unexplored, and to the best of our knowledge, our previous contributions are the only ones in the field.[13] In our previous work, the reaction mechanisms for Au(III)−semisalen catalysts and their Pd(II) analogues were determined and found to be rather similar, except for the role of the solvent. In the case of the Pd catalysts, the solvent is not directly involved in the heterolytic H_2 cleavage step but provides the polar medium that facilitates such a reaction step. In the case of the Au(III)−semisalen complexes, however, the H_2 heterolytic activation was found to take place with the key assistance of a solvent molecule (ethanol). This step generates the active gold−hydride species by releasing one chloride ion and one proton to the bulk.[13]

The aim of the present contribution is to analyze the reaction mechanism for the hydrogenation of alkenes by the catalyst {$(AuCl)_2$[(*R*,*R*)-Me-DuPhos]} by means of theoretical calculations. This complex has neither the capability to act as a metal−ligand bifunctional catalyst (the coordinated ligand is not capable of accommodating a proton) nor the ability to operate by a classical mechanism involving oxidative addition of H_2 along with coordination of the olefin to perform the insertion process. The present study provides a greater understanding of the activation process of the H_2 molecule along with the reaction mechanism for the gold-catalyzed hydrogenation. We checked the literature for the possibility that Au(I) complexes of this type are reduced to nanoparticles by H_2 in situ, but no evidence for this could be found; therefore, this possibility was not considered.

2. COMPUTATIONAL DETAILS AND MODELS

Optimizations were carried out using density functional theory (DFT) with the B3LYP functional,[14] as implemented in Gaussian 03.[15] For the Au atoms, the LANL2DZ pseudopotential[16] was used with the addition of f polarization functions.[17] The 6-31G(d) basis set was used for the C and P atoms, whereas the 6-31+G(d) basis set with additional diffuse functions was used for the O and Cl atoms because of their anionic character. For the H atoms, the 6-31G(d,p) basis set was employed. Solvent effects were included by means of CPCM single-point calculations, though some particular points were fully optimized in solvent.[18] The energies within the text are energies in solution (E_{solv}) unless otherwise stated. Frequency calculations were performed to check for the presence of one imaginary frequency in the transition-state geometries. Extensive preliminary mechanistic analyses were performed using different model systems (see below).

To check whether the account of dispersion interactions played a role, we performed single-point calculations using the M06-L functional[19] for all of the reported stationary points. Moreover, selected transition states were also reoptimized at the same level. In both cases, the single-point M06-L energies and reoptimized geometries were qualitatively comparable to the B3LYP results, indicating that no modification of the mechanistic interpretation was required. It should be noted, however, that most of the hydrogenation energy barriers decreased when the M06-L functional was used, especially those involving relatively bulky substrates (see the Supporting Information). Entropic effects in the gas phase were not included, since they tend to overestimate and underestimate the energetic costs of multimolecular associative and dissociative processes, respectively. We refer to the work by Maseras and coworkers[20] and the references therein for an extended discussion of this topic. Two models of the catalyst were considered: (a) the monometallic complex Me_3P−Au−Cl and (b) a simplified model of the bimetallic {$(AuCl)_2$[(*R*,*R*)-Me-DuPhos]} complex. This allowed us to map the potential energy surface to discover several reaction pathways with a good compromise between accuracy and computational cost. Concerning the substrates, we studied the hydrogenation

dx.doi.org/10.1021/ja305630z | J. Am. Chem. Soc. 2013, 135, 1295−1305

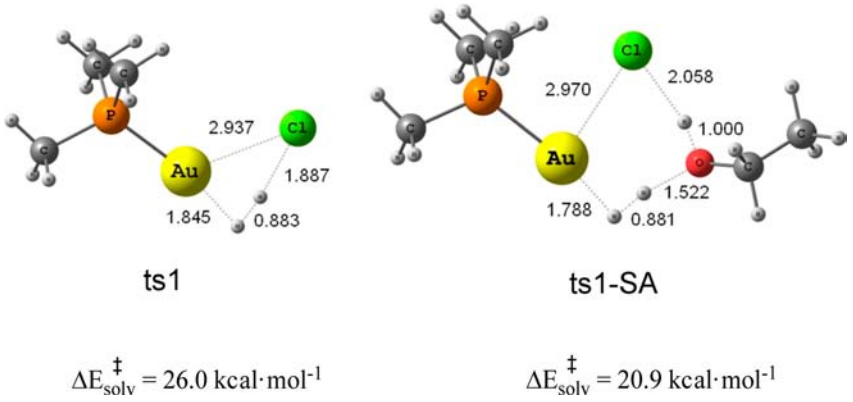

Figure 2. Transition-state structures for heterolytic cleavage of H_2 over the initial gold catalyst without (**ts1**) and with the participation of the solvent (**ts1-SA**). Optimized distances in Å are given.

Scheme 2. Energy Profile for Hydrogenation via Olefin Insertion and Subsequent σ-Bond Metathesis with H_2[a]

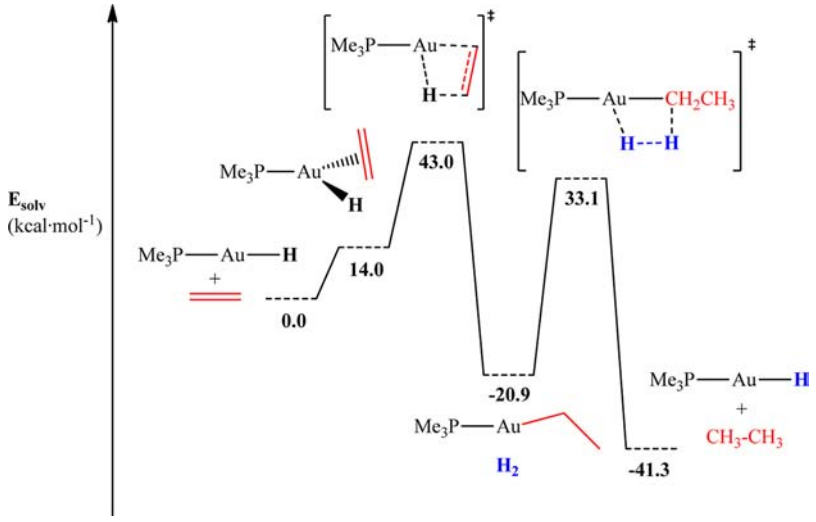

[a] Energies in kcal·mol^{-1} are shown. The olefin is shown in red, and the hydrogens are shown in blue.

reactions with ethene and itaconic acid as simplified models of diethyl 2-benzylidenesuccinate. Structures of the catalyst and substrate models used in the calculations are depicted in Figure 1. In some cases, cyclohexene was also used as a substrate model. Finally, we analyzed the most feasible pathway determined from the models using the complete bimetallic {$(AuCl)_2$[(*R*,*R*)-Me-DuPhos]} catalyst and the experimental substrate diethyl 2-benzylidenesuccinate utilized by Corma and co-workers.[3b]

3. RESULTS AND DISCUSSION

Since the source of hydrogen is H_2, the reaction mechanism must involve hydrogen activation and hydrogenation processes. Molecular hydrogen may be activated in either a homolytic or a heterolytic way.[21] Both possibilities for the activation of H_2 were analyzed here, and we discuss these results first. Subsequently, once the most feasible dihydrogen activation process was determined, several hydrogenation mechanisms were analyzed for different alkenes. The considered processes are classified on the basis of whether the substrate coordinates to the metal catalyst (inner-sphere mechanisms) or not (outer-sphere mechanisms). Next, our evaluation of the step closing the catalytic cycle and regenerating the catalyst is described. Finally, the whole proposed catalytic cycle is discussed. The reaction mechanism is analyzed for both the monometallic and bimetallic catalyst models.

3.1. Au(I) Activation of H_2: Heterolytic or Homolytic?

The homolytic activation would involve a formal oxidative addition and thus would require the metal to have available an oxidation state that is two units higher as well as the capability to coordinate two additional ligands. Conversely, in the heterolytic activation, which would involve a proton transfer to one of the ligands and the formation of a metal−hydride bond, there would be no change in the oxidation state of the metal. The homolytic cleavage of the hydrogen molecule is highly demanding energetically, with an energy barrier of 39.3 kcal·mol^{-1}. The heterolytic activation gives rise to a gold(I)−hydride complex, and the chloride ligand accepts the proton. Despite the fact that gold−hydride species are not very common, they have been reported and suggested as catalytic intermediates.[22] The barrier for the heterolytic activation is 26.0 kcal·mol^{-1} (Figure 2 left). The analogous heterolytic cleavage assisted by a solvent molecule (EtOH) was also analyzed, and as expected, the energy barrier decreased to 20.9 kcal·mol^{-1} (Figure 2 right). In this case, inclusion of the explicit solvent decreased the energy barrier by 5.1 kcal·mol^{-1} with respect to the unassisted process. Several studies have also reported solvent participation in hydrogen heterolytic cleavage and in proton-transfer processes,[23] in line with the present findings. Hence, on the basis of the reported energy barriers, one can

dx.doi.org/10.1021/ja305630z | J. Am. Chem. Soc. 2013, 135, 1295−1305

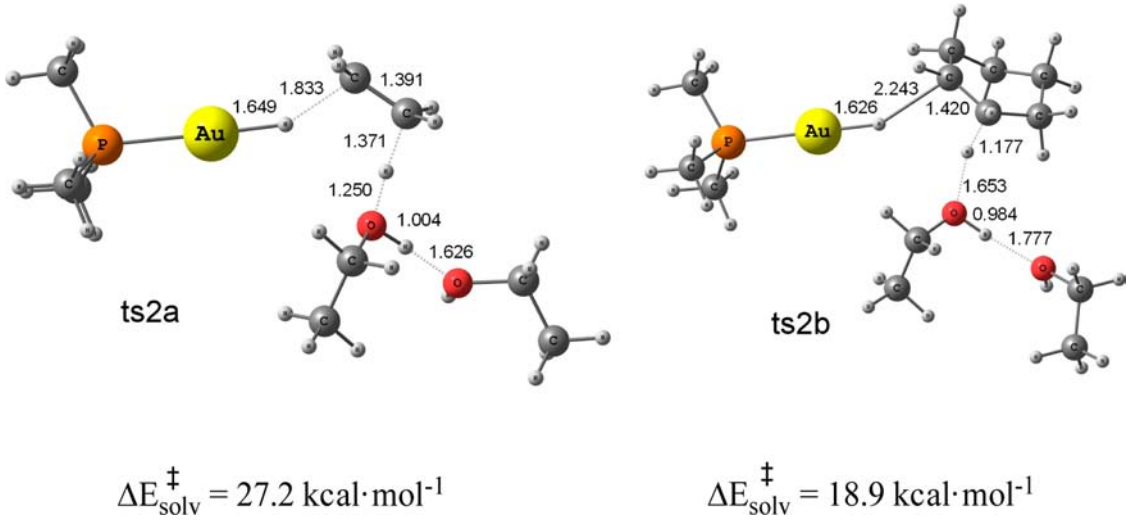

Figure 3. Ionic transition states corresponding to the hydrogenations of ethene (**ts2a**, left) and cyclohexene (**ts2b**, right). Distances in Å are shown.

conclude that the activation of the hydrogen molecule occurs heterolytically. This step generates a Au(I)−hydride complex that can be considered as the active species of the catalyst (see below).

3.2. Hydrogenation Mechanism: Inner-Sphere or Outer-Sphere? As mentioned in the Introduction, hydrogenation processes can be classified on the basis of whether the substrate coordinates to the catalyst (inner-sphere) or not (outer-sphere). For instance, the widely known Wilkinson catalyst for olefin hydrogenation,[24] $RhCl(PPh_3)_3$, operates through an inner-sphere mechanism,[25] while the Ru-based catalyst developed by Noyori and co-workers for asymmetric ketone hydrogenation operates through an outer-sphere pathway.[26]

3.2.1. Inner-Sphere Mechanism. For the present gold catalyst, once the Au−hydride species is generated, the olefin could coordinate to the metal center prior to its insertion into the Au−H bond, which would represent an inner-sphere mechanism. For the monometallic catalyst, insertion of ethylene into the Au−H bond followed by [2 + 2] σ-bond metathesis of an incoming H_2 molecule has an overall energy barrier of 43.0 kcal·mol^{-1} in solution, as shown in Scheme 2.

In addition to this pathway, other inner-sphere mechanisms were also evaluated. The olefin could initially coordinate to the catalyst and then be hydrogenated by the addition of H_2 in two steps through heterolytic activation of the hydrogen molecule (assisted by the solvent). Moreover, other mechanisms in which both gold atoms of the bimetallic model complex participate in a synergistic way were also considered, but they were also too demanding energetically (see the Supporting Information). None of these inner-sphere alternative mechanisms were found to be energetically accessible; hence, outer-sphere alternatives were also evaluated.

3.2.2. Outer-Sphere Mechanisms. The heterolytic activation of H_2 (section 3.1) generates a gold−hydride species together with one proton, which is released to the medium. For this situation, we investigated an outer-sphere hydrogen-transfer mechanism in which the hydride and the proton are transferred to the substrate, with the hydride provided by the metallic species and the proton coming from a protonated solvent molecule.[27] For such a reaction mechanism, coordination of the alkene to the catalyst is not needed for the reaction to proceed. For systems in which both the hydride and the proton come from the catalyst, Noyori coined the expression "bifunctional catalyst".[28] In previous studies of the Ru-based Shvo catalyst, we have shown the preference for this mechanism, though the proton is in that case provided by one CpOH ligand.[7d,9b,27,29] This mechanism is especially preferred over the insertion pathway for hydrogenation of polar double bonds (i.e., ketones and imines). Indeed, for alkene and alkyne hydrogenation it is also preferred over the classical insertion pathway.[9b,29] In the present case, since the proton comes from the solvent, the classification as an ionic mechanism is probably more appropriate.[30] As far as the catalyst is concerned, one or both metal centers can be involved in the mechanism; analyses of these two situations are described in the two following sections.

3.2.2.1. Ionic Mechanism: Monometallic Catalyst. A reaction mechanism involving only one of the gold metal centers in the actual catalyst was analyzed first using the monometallic model catalyst **C1** (Figure 1). These calculations also revealed the feasibility of using the analogous R_3P−Au−Cl monometallic complexes as catalysts.

As previously mentioned, protonated ethanol (formally $EtOH_2^+$) might transfer the proton to the substrate, whereas the hydride would be provided by the activated species of the catalyst, the gold−hydride intermediate. The hydrogen-transfer reaction to ethene has an energy barrier of 27.2 kcal·mol^{-1} within the catalytic cycle.[31] Reoptimization in solution decreased the energy of this transition state by only 0.5 kcal·mol^{-1}, and no significant changes in the optimized structure were observed. The hydrogenation of cyclohexene was also investigated. The relative energy barrier for this substrate was found to be 18.9 kcal·mol^{-1}, and the structure was stabilized by 1.1 kcal·mol^{-1} upon reoptimization in solution. In addition, the energy of the transition state decreased by 7 kcal·mol^{-1} when dispersion effects were included. Hence, the energy barrier decreased significantly compared with ethene as the reactant. This is probably related to the stronger basicity of cyclohexene in comparison with ethene (or, in other words, to the higher stability of the related carbocations, $C_6H_{11}^+$ vs $C_2H_5^+$). In fact, the proton transfer from $EtOH_2^+$ to cyclohexene is greatly favored over the transfer to ethene because the protonation of cyclohexene by $EtOH_2^+$ is endothermic by only 2.4 kcal·mol^{-1}, while for ethene the protonation is endothermic by 13.5 kcal·mol^{-1}. In addition, the energy barrier for the formation of the $C_6H_{11}(EtOH)^+$ species,

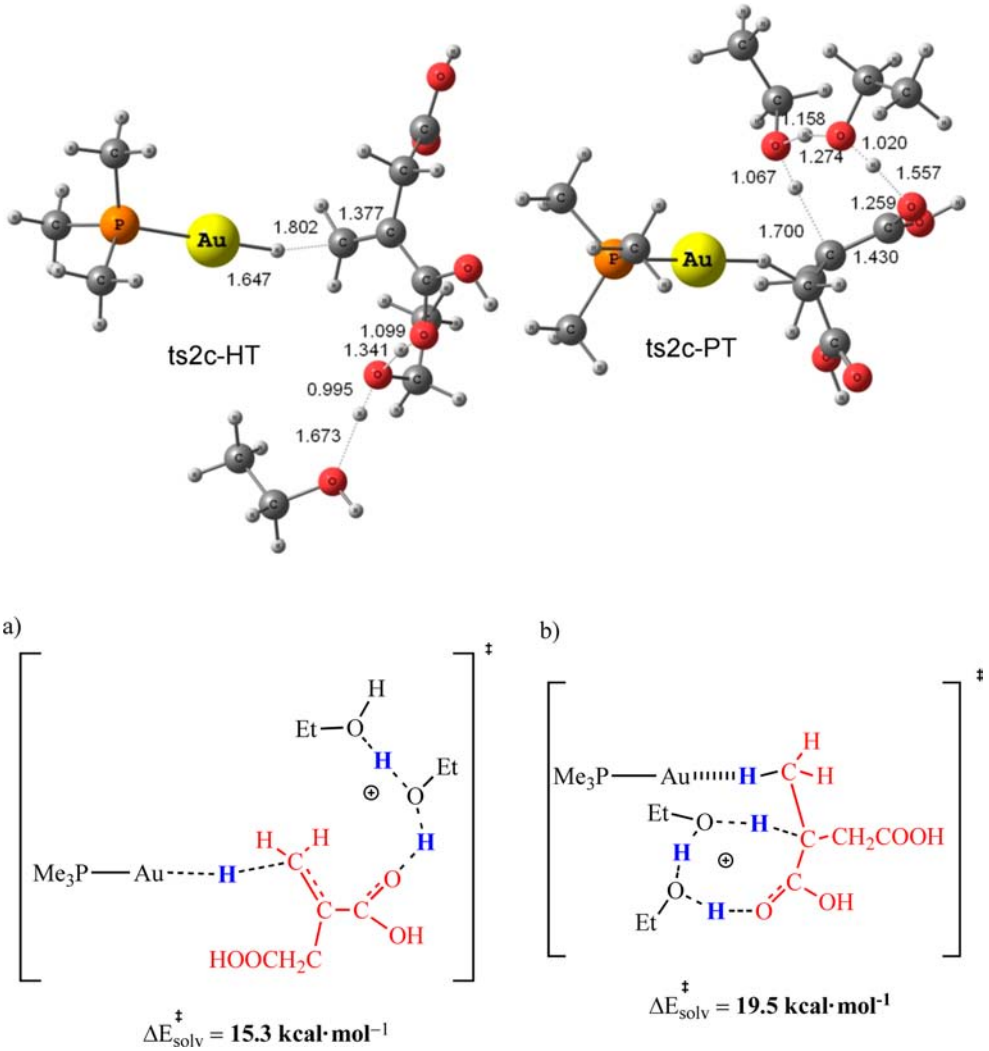

Figure 4. (top) Optimized structures of the two transition-states **ts2c-HT** (left) and **ts2c-PT** (right) leading to the hydrogenation of itaconic acid by means of the monometallic gold catalyst. Optimized distances in Å are given. (bottom) Schematic representations of the transition states for hydrogenation (hydrogens in blue) of itaconic acid (in red) by the monometallic gold catalyst.

which models the proton-transfer step in solution, is only 7.5 kcal·mol^{-1}, and this step is exothermic by 14.3 kcal·mol^{-1}. (Therefore, the hydrogen-transfer mechanism is more feasible for cyclohexene than for ethene). The transition states for the ethene and cyclohexene hydrogenation processes are depicted in Figure 3. The process of forming the new C−H bond by proton transfer from the solvent is more advanced in the transition state in the case of cyclohexene hydrogenation than in the case of ethene hydrogenation (1.177 vs 1.371 Å, respectively). Conversely, the trend for the new C−H bond formed by the hydride transfer is reversed, since the related distances for ethene versus cyclohexene hydrogenation are 1.833 versus 2.243 Å, respectively.

The reaction mechanism for the hydrogenation of a more complex alkene, itaconic acid (model substrate **S2** in Figure 1), was also evaluated. Unexpectedly, the presence of the other functional groups in this alkene led to a change in the reaction mechanism. The new mechanism also involves a hydride transfer and a proton transfer. However, while the hydride is transferred to a carbon of the C═C double bond being hydrogenated, the proton is initially transferred to the oxygen of the C═O bond of the nearer −COOH group, leading to the formation of a $-C(OH)_2^+$ moiety (**ts2c-HT**) (Figure 4). This transition state has an energy barrier within the catalytic cycle of only 15.3 kcal·mol^{-1} (see section 3.3 for the discussion of the active species of the catalyst). The decrease in the barrier height for the hydrogen-transfer process is also mainly due to the more favored protonation of the substrate. In this case, the proton transfer from $EtOH_2^+$ to one oxygen of the −COOH group of itaconic acid is practically isothermic (0.6 kcal·mol^{-1}). In a second step, an intramolecular proton transfer (assisted by two solvent molecules) from the $-C(OH)_2^+$ moiety to the unsaturated carbon of the initial C═C double bond (**ts2c-PT**) gives rise to the hydrogenated product. A similar solvent-assisted proton-transfer step has also recently been proposed for the gold-catalyzed hydration of alkynes.[12P] In the structure of **ts2c-PT**, the substrate is coordinated to the catalyst. The energy barrier within the catalytic cycle is 19.5 kcal·mol^{-1}. Moreover, the transition state was stabilized by 2.5 kcal·mol^{-1} upon optimization in solution and by ∼10 kcal·mol^{-1} when dispersion effects were included. This is an affordable energy profile for the reaction mechanism of this substrate. Thus, according to the calculations, R_3P−Au−Cl should be also a catalyst for alkene hydrogenations.

3.2.2.2. Ionic Mechanism: Bimetallic Catalyst. The ionic mechanism was also studied by considering the catalyst as a

dx.doi.org/10.1021/ja305630z | J. Am. Chem. Soc. 2013, 135, 1295−1305

bimetallic system where both metal centers can actively participate in the process. The cooperation of two metallic centers for catalysis is starting to be proposed in the literature.[32] Several alternatives were analyzed (see the Supporting Information), and we describe here the most feasible one. For cyclohexene and ethene hydrogenation, we obtained lower energy barriers than for the monometallic system. For the case of cyclohexene, the energy barrier was reduced to 9.9 kcal·mol^{-1} with respect to the active catalytic species. In the related transition-state structure **ts2d** (Figure 5), the cyclohexene is formally protonated since the new C−H bond is already formed (1.096 Å); the imaginary frequency in **ts2d** confirmed that *only* the hydride is being transferred at this stage and that the proton has already been completely transferred to the substrate. We found analogous results for the case of ethene hydrogenation. Thus, these results suggest that alkene hydrogenation by means of the bimetallic gold catalyst involves a *stepwise* hydrogen transfer mechanism in which the proton transfer is followed by the hydride transfer to the substrate.

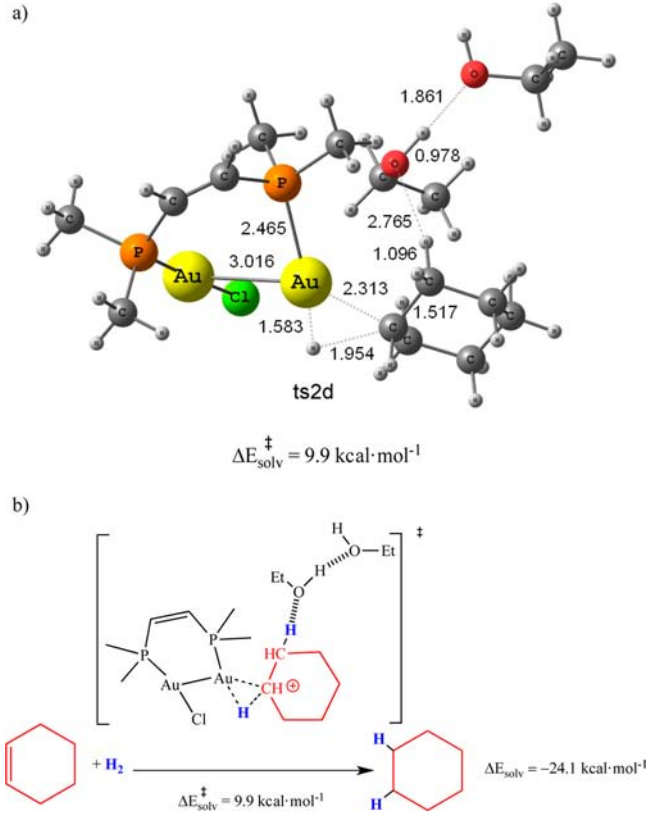

Figure 5. (a) Optimized structure of transition state **ts2d** corresponding to the hydrogenation of cyclohexene catalyzed by the bimetallic system. Optimized distances in Å are given. (b) Schematic representation of the calculated reaction pathway and transition state.

Such behavior is similar to that found for the outer-sphere hydrogenation of alkenes and imines catalyzed by the Ru-based Shvo catalyst. In that case, the related transition state for the imine hydrogenation also mainly involves *hydride* transfer to the carbon of the C=N double bond.[9b,27,29] Privalov and Bäckvall also proposed a *fast* proton transfer and a *slow* hydride transfer in the inner-sphere mechanism for imine hydrogenation by the same Ru-based catalyst.[33]

The most feasible pathway for both the monometallic and bimetallic catalysts involves an ionic mechanism. Moreover, when the analogous reaction steps in the hydrogenations of cyclohexene by the monometallic and bimetallic systems are compared, the bimetallic complex shows a lower energy barrier than the monometallic system: 9.9 kcal·mol^{-1} for **ts2d** versus 18.9 kcal·mol^{-1} for **ts2b**. Moreover, the former structure is more stable than the latter by 7 kcal·mol^{-1} when dispersion effects are included. The reaction mechanism for the bimetallic system is slightly different, since prior to the hydride transfer to the substrate the protonated cyclohexene interacts with the catalyst to form an intermediate that easily evolves to products with a relative energy barrier of only 2.5 kcal·mol^{-1}. The analogous intermediate for the case of the monometallic catalyst was not found. The energy barrier for the initial cyclohexene protonation is only 7.5 kcal·mol^{-1}. Overall, the energy barrier for the hydrogenation step is significantly reduced in the case of the bimetallic catalyst. The final products are cyclohexane and the $[(PMe_2CH)_2Au_2Cl]^+$ complex. The Au−Au distance is 2.857 Å in the latter species; reoptimization using the M06-L functional showed a short Au−Au distance of 2.835 Å, thus suggesting an aurophilic interaction.[34]

The hydrogenation of itaconic acid using the binuclear Au model catalyst was also investigated. Hydride transfers for two different situations were considered: when the proton was transferred to the C=C double bond (**ts2d-HT-1**) or to the COOH group (**ts2d-HT-2**) (Figure 6). The transition state in which the proton was already transferred to the C=C double bond (rather than to the −COOH group) was more favorable by ∼8 kcal·mol^{-1}. Within the catalytic cycle, the related energy barriers in solution ($\Delta E^{\ddagger}_{solv}$) were 13.9 and 22.2 kcal·mol^{-1}, respectively, and they were stabilized by 5 and 15 kcal·mol^{-1}, respectively, when evaluated using the M06-L functional. Both transition-state structures are depicted in Figure 6. When comparing the two structures, one can observe that **ts2d-HT-1** *resembles* an eliminative reduction step from a square-planar complex while **ts2d-HT-2** involves hydride transfer without substrate coordination. It should be noted that the energy barriers are approximate in the sense that the substrate may adopt several conformations, which may lead to lower energy barriers; however, both pathways are possible and show the feasibility of the ionic mechanism.

As we previously estimated, protonation of the −COOH group of itaconic acid from the solvent ($EtOH_2^+$) can take place easily since this process is endothermic by only 0.6 kcal·mol^{-1}. Thus, for this substrate (and also for the case of the monometallic catalyst), a second step involving the intramolecular solvent-assisted proton transfer from the $-C(OH)_2^+$ group to the unsaturated carbon of the initial C=C double bond is required in order to complete the hydrogenation reaction. Since this is the step that creates the chiral center, it was evaluated using the complete catalyst and diethyl 2-benzylidenesuccinate as the substrate (see section 3.4)

3.3. Catalyst Regeneration. The reaction mechanism presented above gives rise to the hydrogenated product and the formation of a cationic form of the catalyst. The vacancy generated by release of the product is occupied by a solvent molecule (EtOH); this intermediate is located 13.8 kcal·mol^{-1} above the initial reactants. Such a cationic species can form the hydride intermediate by heterolytic cleavage of an H_2 molecule (Figure 7).

Heterolytic cleavage of the H_2 molecule gives rise to the gold−hydride intermediate and $EtOH_2^+$. In this case, the related transition state is located 12.6 kcal·mol^{-1} above the

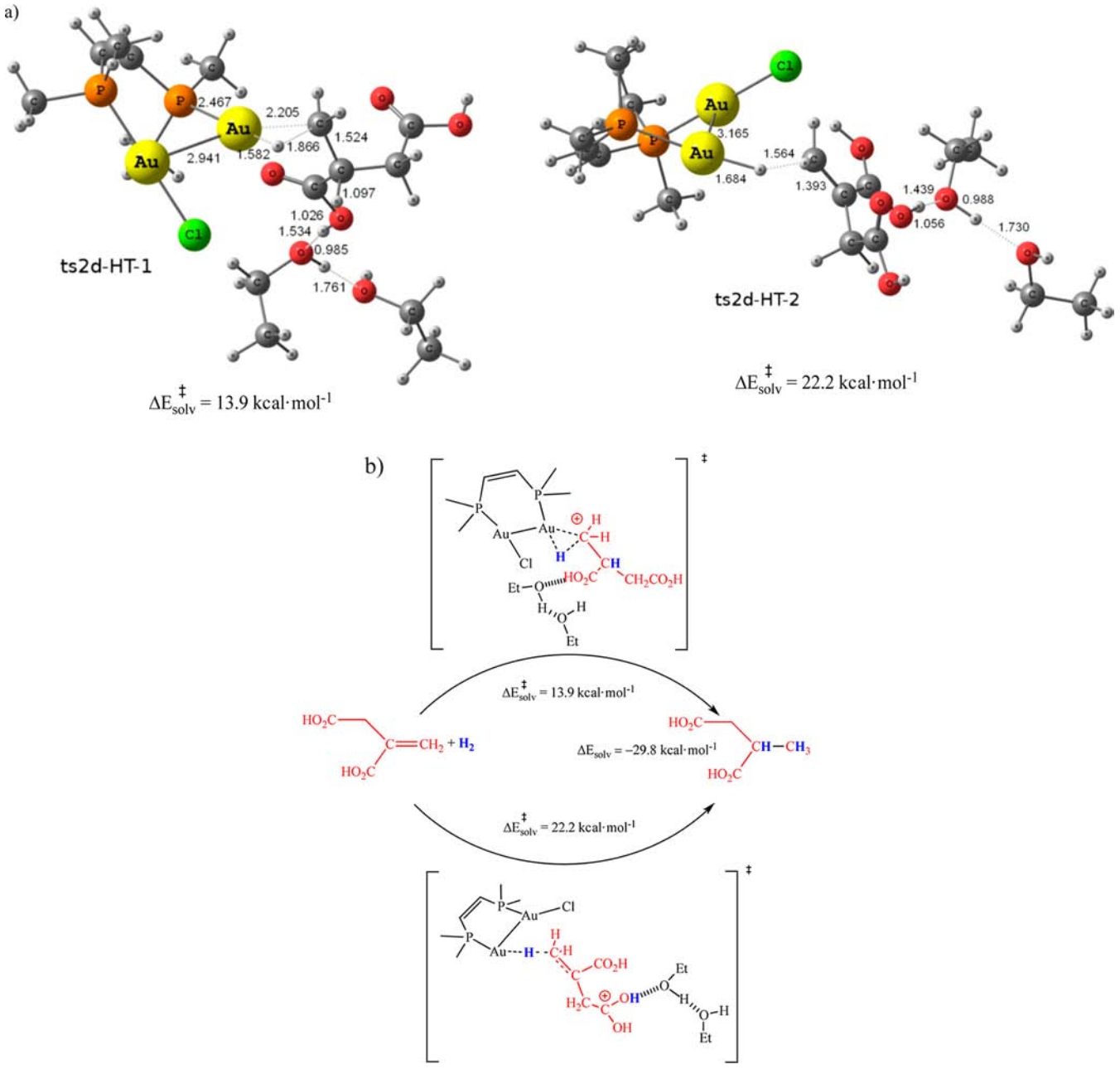

Figure 6. (a) Transition-state structures for the hydride transfer when itaconic acid is protonated on either the initial C═C bond (**ts2d-HT-1**, left) or the −COOH group (**ts2d-HT-2**, right). Optimized distances in Å are given. (b) Schematic representations of the calculated reaction pathways and the related transition states.

$[Me_3P–Au–OHEt]^+$ intermediate, which is more stable than the $Me_3P–Au–H$ species by 11.7 kcal·mol^{-1}. The $[Me_3P–Au–OHEt]^+$ species has the lowest energy within the catalytic cycle, and hence, energies within the catalytic cycle are given relative to this species (or an analogous one for the bimetallic cases) plus one additional EtOH molecule. For the catalyst regeneration step, including two ethanol molecules in the calculations instead of one did not modify the energy barrier significantly. The transition-state structures (**ts3** and **ts4**) are shown in Figure 7.

3.4. Ionic Mechanism for the Complete Catalyst. Finally, we evaluated the most plausible mechanism for the hydrogenation of itaconic acid using the complete catalyst, $\{(AuCl)_2[(R,R)$-Me-DuPhos$]\}$. Hence, the intramolecular proton-transfer process depending on the coordination of the substrate to the metal catalyst was analyzed. According to our results for the monometallic system, the intramolecular proton transfer is the step that most likely determines the enantioselectivity in the hydrogenation of itaconic acid (**ts2c-PT** in Figure 4).

Hence, we evaluated this proton transfer for the complete bimetallic catalyst. We characterized several transition states for the solvent-assisted intramolecular proton transfer that differed with respect to the coordination mode of the substrate (Figure 8): one with the substrate coordinated through the OH group from the previously formed $-C(OH)_2^+$ moiety (**ts2d-PT**), another coordinated by means of the oxygen of the −COOH group (**ts2d-PT′**), and finally a third one coordinated through the newly formed C–H bond resulting from the hydride transfer (**ts2d-PT″**). These were the most stable configurations

dx.doi.org/10.1021/ja305630z | J. Am. Chem. Soc. 2013, 135, 1295−1305

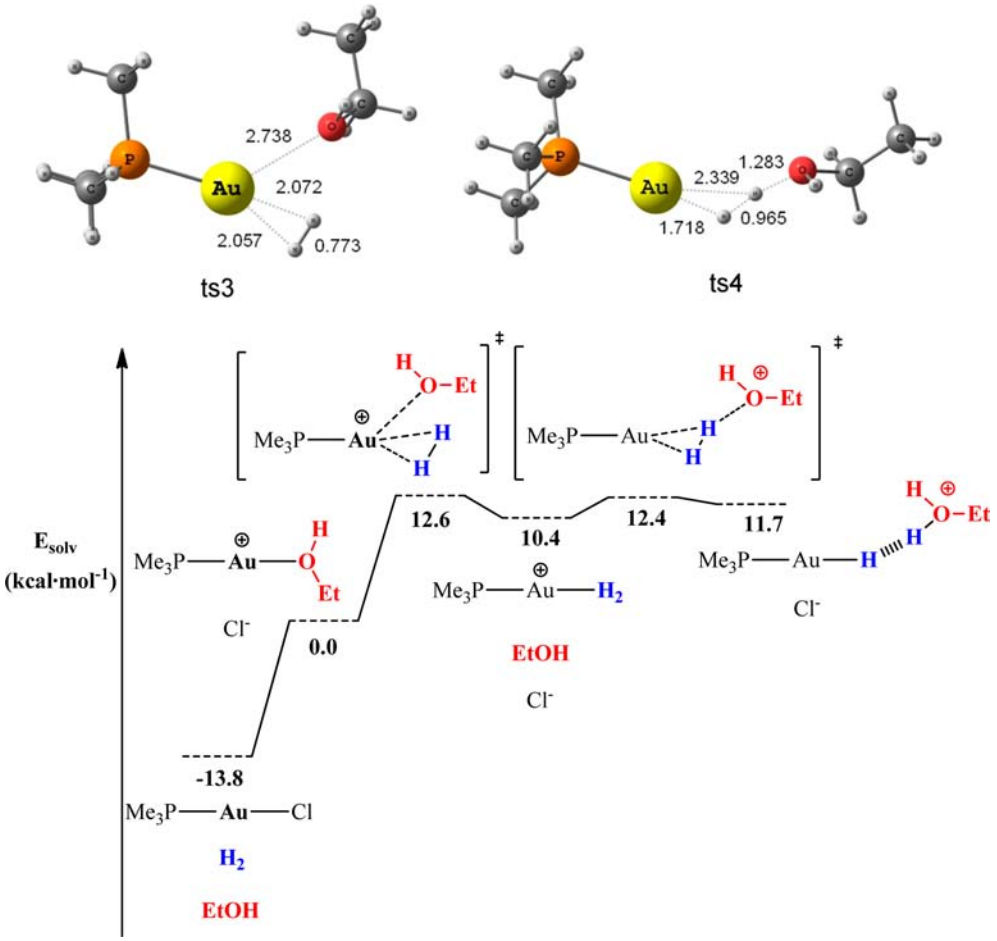

Figure 7. (top) Transition-state structures involved in hydride regeneration: (left) **ts3** for substitution of the ethanol molecule by a hydrogen molecule; (right) **ts4** for heterolytic cleavage of the hydrogen molecule to form the gold–hydride complex and protonated solvent. Distances in Å are shown. (bottom) Energy profile of the proposed pathway for the regeneration of the metal–hydride complex involving heterolytic cleavage of H_2 (in blue) by means of EtOH (in red).

characterized during the transition-state search (Figure 8). The last transition state, **ts2d-PT″**, corresponds to a pathway with no change in the coordination mode of the substrate after the hydride transfer. Its relative energy, however, is 18.3 kcal·mol^{-1} higher than that for the most stable proton-transfer transition state, **ts2d-PT**, which has the substrate coordinated to the catalyst through the $-C(OH)_2^+$ moiety; the coordinating OH group is the one involved in the proton transfer.

After determining the most stable transition state with respect to the coordination mode of the substrate, we studied the intramolecular proton-transfer step for diethyl 2-benzylidenesuccinate, the experimental alkene used by Corma and coworkers.[3b] The catalyst used for the calculations was the complete {$(AuCl)_2$[(*R*,*R*)-Me-DuPhos]} structure. In this case, we located the most stable transition state for proton transfer assisted by two ethanol molecules (Figure 9). This structure, **ts2e-PT**, is analogous to the **ts2d-PT** structure shown in Figure 8, and it is the transition state for the last step in the hydrogenation of diethyl 2-benzylidenesuccinate catalyzed by the complete bimetallic catalyst {$(AuCl)_2$[(*R*,*R*)-Me-DuPhos]}. The enantioselectivity-determining step of the diethyl 2-benzylidenesuccinate hydrogenation catalyzed by the {$(AuCl)_2$[(*R*,*R*)-Me-DuPhos]} complex is located at 23.2 kcal·mol^{-1} relative to the initial reactants, while the energy barrier within the catalytic cycle is only 9.2 kcal·mol^{-1}.

The proposed catalytic cycle derived from our DFT calculations is summarized in Scheme 3. The reaction starts with the formation of the gold–hydride species through heterolytic cleavage of the hydrogen molecule.[13] This species is the one involved in the first catalytic cycle. Next, the hydride is transferred to the unsaturated carbon and the proton is transferred to the CO_2Et group contiguous to the C=C double bond (**ts2d-HT-2**) or to the other carbon of the C=C double bond of diethyl 2-benzylidenesuccinate (**ts2d-HT-1**). This process probably occurs in a *stepwise* fashion starting with the proton transfer, as suggested by the nature of the transition state and experience with related processes.[7d,9b,29] The proton may not be directly transferred to the carbon of the initial C=C double bond but instead could be transferred to the O atom in the C=O double bond of the nearer COOEt substituent of the alkene. It should be noted that the proton is provided by the medium (protonated ethanol). In the case where the proton is transferred to the O atom, such proton transfer to the initial substrate is feasible, as it is nearly isothermic. After a change in the coordination mode of the partially hydrogenated substrate to the gold center from the C–H agostic mode to the most stable coordination through the OH ligand, the proton is intramolecularly transferred to the unsaturated carbon of the initial C=C double bond, generating the chiral center. At the end, the gold–hydride species is

dx.doi.org/10.1021/ja305630z | *J. Am. Chem. Soc.* 2013, 135, 1295–1305

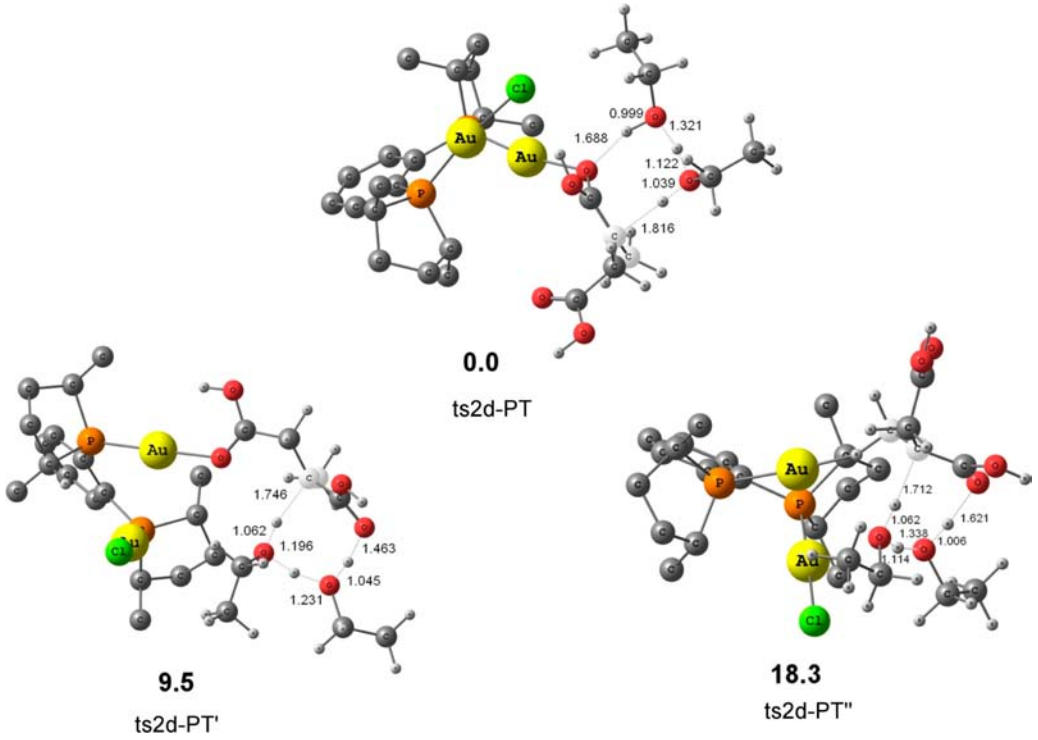

Figure 8. Transition-state structures **ts2d-PT**, **ts2d-PT′**, and **ts2d-PT″** for the intramolecular solvent-assisted proton-transfer step. The structures differ with respect to the mode of coordination of the alkyl species to the active catalyst. The hydrogens of the phosphine ligands have been omitted for clarity; the initial C═C bond is shown in white. Relative energies in kcal·mol^{-1} and distances in Å are shown.

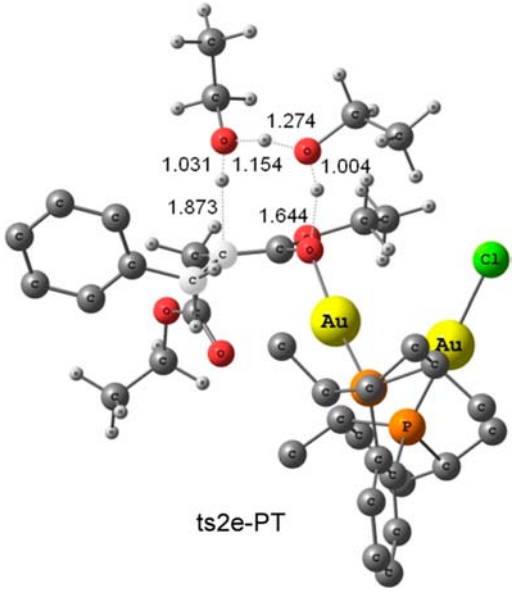

Figure 9. Transition state **ts2e-PT** for the final solvent-assisted intramolecular proton transfer in the hydrogenation of diethyl 2-benzylidenesuccinate catalyzed by {(AuCl)$_2$[(*R*,*R*)-Me-DuPhos]}. The hydrogens of the DuPhos ligand have been omitted for clarity, and the initial C═C bond is shown in white. Distances in Å are given.

regenerated by heterolytic cleavage of an incoming H_2 molecule with release of a proton to the medium (ethanol), as described in section 3.3.

4. CONCLUSIONS

The hydrogen activation in the case of the catalyst {(AuCl)$_2$[(*R*,*R*)-Me-DuPhos]} takes place heterolytically, generating the active gold hydride catalytic species along with a proton and a chloride ion, which end up in the medium, in agreement with our previous study.[3] In this case, after the generation of the gold−hydride species, the hydrogenation proceeds through an ionic mechanism. This mechanism involves the net addition of one H_2 molecule through transfer of one proton (H^+) and one hydride (H^-) to the alkene. The proton comes from the solvent (protonated ethanol), while the hydride comes from the gold−hydride intermediate. This spreads the ionic mechanism term to gold catalysts, providing useful insights for the fundamental understanding of gold-catalyzed homogeneous hydrogenations. In the present case, we also noticed that the solvent is not a mere spectator but rather helps both in the heterolytic cleavage of the H_2 molecule and in the hydrogenation itself within the catalytic cycle. According to our proposed mechanism, polar and slightly acidic media are expected to facilitate gold-catalyzed hydrogenations. When comparing the bimetallic and monometallic systems for cyclohexene hydrogenation, we found that *only* the hydride transfer is occurring at the transition state. Analogous results were found for ethene hydrogenation. According to the Au−Au distance for the active cationic gold complex, aurophilicity could be at play in the bimetallic system. Hence, for the bimetallic gold catalyst, our data suggest a stepwise reaction mechanism in which the proton transfer is followed by the hydride transfer. Finally, for the hydrogenation of diethyl benzylidenesuccinate, the hydride and the proton are also transferred to the substrate. However, the proton initially could be directly transferred not to one of the unsaturated carbon atoms but rather to the CO_2Et substituent contiguous to the initial C═C double bond. In this case, an additional intramolecular proton transfer assisted by the solvent is required in order to complete the hydrogenation reaction.

dx.doi.org/10.1021/ja305630z | *J. Am. Chem. Soc.* 2013, 135, 1295−1305

Scheme 3. Proposed Catalytic Cycle for the Enantioselective Hydrogenation of Diethyl 2-Benzylidenesuccinate Catalyzed by {$(AuCl)_2$[(*R*,*R*)-Me-DuPhos]}[a]

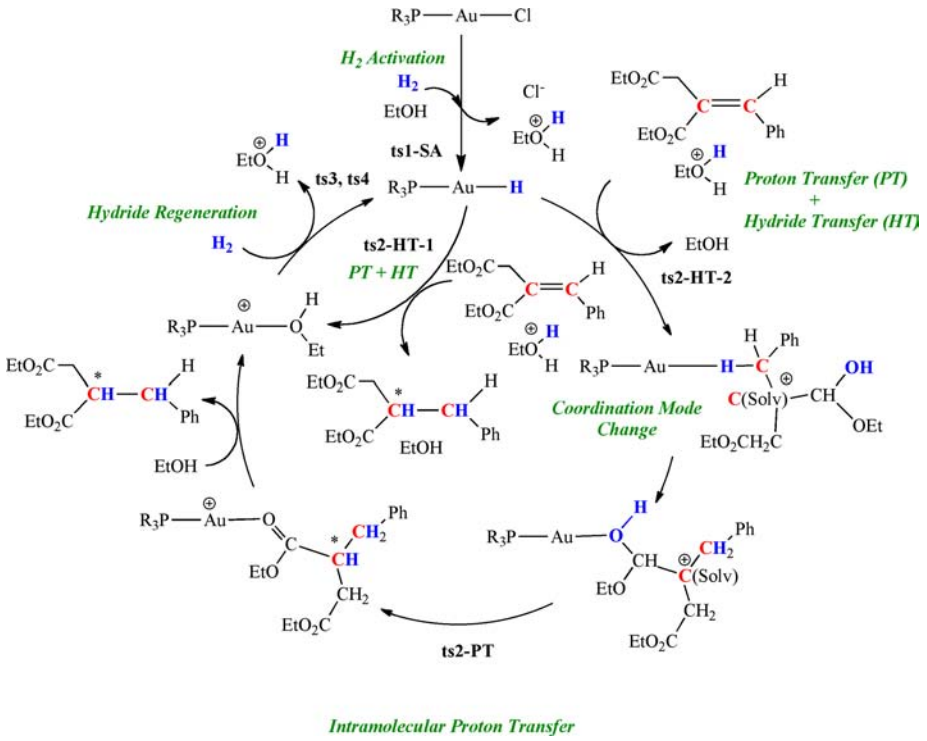

[a]The hydrogens coming from the H_2 molecule and the carbons of the initial C═C bond are highlighted in blue and red, respectively.

Our data suggest that the step determining the enantioselectivity involves a proton transfer to the prochiral carbon. Further investigations are being carried out in order to determine whether the ionic mechanism can be extended to other gold-catalyzed hydrogenations in particular and to other transition-metal-catalyzed hydrogenations in general.

■ ASSOCIATED CONTENT

Supporting Information

Additional calculated reaction pathways, energetic influence of the number of solvent (EtOH) molecules included in the model, comparison between B3LYP and M06-L methods, and absolute energies and coordinates of the optimized geometries. This material is available free of charge via the Internet at http://pubs.acs.org.

■ AUTHOR INFORMATION

Corresponding Author

comas@inorg.chem.ethz.ch; gregori@klingon.uab.es

Notes

The authors declare no competing financial interest.

■ ACKNOWLEDGMENTS

We are grateful to the Spanish MICINN (Projects CTQ2011-23336, Consolider Ingenio 2010 CSD2007-00006, FPU fellowship to A.C.-V.) and to Generalitat de Catalunya (2009/SGR/68; XRQTC). We also thank Avelino Corma, Marta Iglesias, and Félix Sánchez for fruitful discussions.

■ REFERENCES

(1) (a) Hashmi, A. S. K.; Hutchings, G. J. *Angew. Chem., Int. Ed.* **2006**, *45*, 7896−7936. (b) Gorin, D. J.; Sherry, B. D.; Toste, F. D. *Chem. Rev.* **2008**, *108*, 3351−3378. (c) Hashmi, A. S. K.; Rudolph, M. *Chem. Soc. Rev.* **2008**, *37*, 1766−1775. (d) Li, Z. G.; Brouwer, C.; He, C. *Chem. Rev.* **2008**, *108*, 3239−3265. (e) Arcadi, A. *Chem. Rev.* **2008**, *108*, 3266−3325. (f) Jiménez-Núñez, E.; Echavarren, A. M. *Chem. Rev.* **2008**, *108*, 3326−3350. (g) Zhang, J. L.; Yang, C. G.; He, C. *J. Am. Chem. Soc.* **2006**, *128*, 1798−1799. (h) Fructos, M. R.; Belderrain, T. R.; de Fremont, P.; Scott, N. M.; Nolan, S. P.; Diaz-Requejo, M. M.; Perez, P. J. *Angew. Chem., Int. Ed.* **2005**, *44*, 5284−5288. (i) Gonzalez-Arellano, C.; Corma, A.; Iglesias, M.; Sanchez, F. *Chem. Commun.* **2005**, 1990−1992. (j) Gonzalez-Arellano, C.; Corma, A.; Iglesias, M.; Sanchez, F. *J. Catal.* **2006**, *238*, 497−501. (k) Giner, X.; Najera, C. *Org. Lett.* **2008**, *10*, 2919−2922. (l) Antoniotti, S.; Genin, E.; Michelet, V.; Genêt, J.-P. *J. Am. Chem. Soc.* **2005**, *127*, 9976−9977. (m) Giner, X.; Nájera, C.; Kovács, G.; Lledós, A.; Ujaque, G. *Adv. Synth. Catal.* **2011**, *353*, 3451−3466. (n) Rudolph, M.; Hashmi, A. S. K. *Chem. Soc. Rev.* **2012**, *41*, 2448−2462. (o) Cardenas-Lizana, F.; Keane, M. A. *J. Mater. Sci.* **2012**, DOI: 10.1007/s10853-012-6766-7.

(2) Ito, Y.; Sawamura, M.; Hayashi, T. *J. Am. Chem. Soc.* **1986**, *108*, 6405−6406.

(3) (a) Echavarren, A. M.; Munoz, M. P.; Adrio, J.; Carretero, J. C. *Organometallics* **2005**, *24*, 1293−1300. (b) Gonzalez-Arellano, C.; Corma, A.; Iglesias, M.; Sanchez, F. *Chem. Commun.* **2005**, 3451−3453. (c) Widenhoefer, R. A. *Chem.—Eur. J.* **2008**, *14*, 5382−5391. (d) Alonso, I.; Trillo, B.; López, F.; Montserrat, S.; Ujaque, G.; Castedo, L.; Lledós, A.; Mascareñas, J. L. *J. Am. Chem. Soc.* **2009**, *131*, 13020−13030.

(4) (a) Gladiali, S.; Alberico, E. *Chem. Soc. Rev.* **2006**, *35*, 226−236. (b) Samec, J. S. M.; Bäckvall, J.-E.; Andersson, P. G.; Brandt, P. *Chem. Soc. Rev.* **2006**, *35*, 237−248. (c) *Handbook of Homogeneous Hydrogenation*; de Vries, J. G., Elsevier, C. J., Eds.; Wiley-VCH: Weinheim, Germany, 2007. (d) Clapham, S. E.; Hadzovic, A.; Morris, R. H. *Coord. Chem. Rev.* **2004**, *248*, 2201−2237.

(5) Sandoval, C. A.; Ohkuma, T.; Muniz, K.; Noyori, R. *J. Am. Chem. Soc.* **2003**, *125*, 13490−13503.

(6) Abdur-Rashid, K.; Clapham, S. E.; Hadzovic, A.; Harvey, J. N.; Lough, A. J.; Morris, R. H. *J. Am. Chem. Soc.* **2002**, *124*, 15104−15118.

(7) (a) Casey, C. P.; Bikzhanova, G. A.; Cui, Q.; Guzei, I. A. *J. Am. Chem. Soc.* **2005**, *127*, 14062−14071. (b) Alonso, D. A.; Brandt, P.; Nordin, S. J. M.; Andersson, P. G. *J. Am. Chem. Soc.* **1999**, *121*, 9580−9588. (c) Guo, X.; Tang, Y.; Zhang, X.; Lei, M. *J. Phys. Chem. A* **2011**, *115*, 12321−12330. (d) Comas-Vives, A.; Ujaque, G.; Lledós, A. *Organometallics* **2007**, *26*, 4135−4144.
(8) Yang, X.; Zhao, L.; Fox, T.; Wang, Z.-X.; Berke, H. *Angew. Chem., Int. Ed.* **2010**, *49*, 2058−2062.
(9) (a) Shvo, Y.; Goldberg, I.; Czerkie, D.; Reshef, D.; Stein, Z. *Organometallics* **1997**, *16*, 133−138. (b) Comas-Vives, A.; Ujaque, G.; Lledós, A. *Organometallics* **2008**, *27*, 4854−4863.
(10) Dobereiner, G. E.; Nova, A.; Schley, N. D.; Hazari, N.; Miller, S. J.; Eisenstein, O.; Crabtree, R. H. *J. Am. Chem. Soc.* **2011**, *133*, 7547−7562.
(11) (a) Morokuma, K.; Musaev, D. G. *Computational Modeling for Homogeneous and Enzymatic Catalysis: A Knowledge Data Base for Designing Efficient Catalysts*; Wiley-VCH: Weinheim, Germany, 2008. (b) Lledós, A.; Maseras, F. *Computational Modeling of Homogeneous Catalysis*; Kluwer Academic Publishers: Dordrecht, The Netherlands, 2002. (c) Borden, W. T. *J. Am. Chem. Soc.* **2011**, *133*, 14841−14843.
(12) (a) Pyykkö, P. *Inorg. Chim. Acta* **2005**, *358*, 4113−4130. (b) Pyykkö, P. *Chem. Soc. Rev.* **2008**, *37*, 1967−1997. (c) Cuenca, A. B.; Montserrat, S.; Hossain, K. M.; Mancha, G.; Lledós, A.; Medio-Simon, M.; Ujaque, G.; Asensio, G. *Org. Lett.* **2009**, *11*, 4906−4909. (d) Kovacs, G.; Ujaque, G.; Lledós, A. *J. Am. Chem. Soc.* **2008**, *130*, 853−864. (e) Trillo, B.; López, F.; Montserrat, S.; Ujaque, G.; Castedo, L.; Lledós, A.; Mascareñas, J. L. *Chem.—Eur. J.* **2009**, *15*, 3336−3339. (f) Gorin, D. J.; Toste, F. D. *Nature* **2007**, *446*, 395−403. (g) Furstner, A.; Davies, P. W. *Angew. Chem., Int. Ed.* **2007**, *46*, 3410−3449. (h) Nieto-Oberhuber, C.; Lopez, S.; Munoz, M. P.; Cardenas, D. J.; Bunuel, E.; Nevado, C.; Echavarren, A. M. *Angew. Chem., Int. Ed.* **2005**, *44*, 6146−6148. (i) Gandon, V.; Lemiere, G.; Hours, A.; Fensterbank, L.; Malacria, M. *Angew. Chem., Int. Ed.* **2008**, *47*, 7534−7538. (j) Correa, A.; Marion, N.; Fensterbank, L.; Malacria, M.; Nolan, S. P.; Cavallo, L. *Angew. Chem., Int. Ed.* **2008**, *47*, 718−721. (k) Lemiere, G.; Gandon, V.; Agenet, N.; Goddard, J. P.; de Kozak, A.; Aubert, C.; Fensterbank, L.; Malacria, M. *Angew. Chem., Int. Ed.* **2006**, *45*, 7596−7599. (l) Faza, O. N.; Lopez, C. S.; Alvarez, R.; de Lera, A. R. *J. Am. Chem. Soc.* **2006**, *128*, 2434−2437. (m) Montserrat, S.; Ujaque, G.; López, F.; Mascareñas, J. L.; Lledós, A. *Top. Curr. Chem.* **2011**, *302*, 225−248. (n) Lein, M.; Rudolph, M.; Hashmi, S. K.; Schwerdtfeger, P. *Organometallics* **2010**, *29*, 2206−2210. (o) Pernpointner, M.; Hashmi, A. S. K. *J. Chem. Theory Comput.* **2009**, *5*, 2717−2725. (p) Krauter, C. M.; Hashmi, A. S. K.; Pernpointner, M. *ChemCatChem* **2010**, *2*, 1226−1230. (q) Hashmi, A. S. K.; Schuster, A. M.; Litters, S.; Rominger, F.; Pernpointner, M. *Chem.—Eur. J.* **2011**, *17*, 5661−5667. (r) Hashmi, A. S. K.; Pernpointner, M.; Hansmann, M. M. *Faraday Discuss.* **2011**, *152*, 179−184. (s) Döpp, R.; Lothschütz, C.; Wurm, T.; Pernpointner, M.; Keller, S.; Rominger, F.; Hashmi, A. S. K. *Organometallics* **2011**, *30*, 5894−5903.
(13) (a) Comas-Vives, A.; Gonzalez-Arellano, C.; Corma, A.; Iglesias, M.; Sanchez, F.; Ujaque, G. *J. Am. Chem. Soc.* **2006**, *128*, 4756−4765. (b) Comas-Vives, A.; Gonzalez-Arellano, C.; Boronat, M.; Corma, A.; Iglesias, M.; Sanchez, F.; Ujaque, G. *J. Catal.* **2008**, *254*, 226−237.
(14) (a) Becke, A. D. *J. Chem. Phys.* **1993**, *98*, 5648−5652. (b) Lee, C. T.; Yang, W. T.; Parr, R. G. *Phys. Rev. B* **1988**, *37*, 785−789. (c) Stephens, P. J.; Devlin, F. J.; Chabalowski, C. F.; Frisch, M. J. *J. Phys. Chem.* **1994**, *98*, 11623−11627.
(15) Frisch, M. J.; Trucks, G. W.; Schlegel, H. B.; Scuseria, G. E.; Robb, M. A.; Cheeseman, J. R.; Montgomery, J. A., Jr.; Vreven, T.; Kudin, K. N.; Burant, J. C.; Millam, J. M.; Iyengar, S. S.; Tomasi, J.; Barone, V.; Mennucci, B.; Cossi, M.; Scalmani, G.; Rega, N.; Petersson, G. A.; Nakatsuji, H.; Hada, M.; Ehara, M.; Toyota, K.; Fukuda, R.; Hasegawa, J.; Ishida, M.; Nakajima, T.; Honda, Y.; Kitao, O.; Nakai, H.; Klene, M.; Li, X.; Knox, J. E.; Hratchian, H. P.; Cross, J. B.; Bakken, V.; Adamo, C.; Jaramillo, J.; Gomperts, R.; Stratmann, R. E.; Yazyev, O.; Austin, A. J.; Cammi, R.; Pomelli, C.; Ochterski, J. W.; Ayala, P. Y.; Morokuma, K.; Voth, G. A.; Salvador, P.; Dannenberg, J. J.; Zakrzewski, V. G.; Dapprich, S.; Daniels, A. D.; Strain, M. C.; Farkas, O.; Malick, D. K.; Rabuck, A. D.; Raghavachari, K.; Foresman, J. B.; Ortiz, J. V.; Cui, Q.; Baboul, A. G.; Clifford, S.; Cioslowski, J.; Stefanov, B. B.; Liu, G.; Liashenko, A.; Piskorz, P.; Komaromi, I.; Martin, R. L.; Fox, D. J.; Keith, T.; Al-Laham, M. A.; Peng, C. Y.; Nanayakkara, A.; Challacombe, M.; Gill, P. M. W.; Johnson, B.; Chen, W.; Wong, M. W.; Gonzalez, C.; Pople, J. A. *Gaussian 03*, revision C.02; Gaussian, Inc.: Wallingford, CT, 2004.
(16) Hay, P. J.; Wadt, W. R. *J. Chem. Phys.* **1985**, *82*, 270−283.
(17) Ehlers, A. W.; Bohme, M.; Dapprich, S.; Gobbi, A.; Hollwarth, A.; Jonas, V.; Kohler, K. F.; Stegmann, R.; Veldkamp, A.; Frenking, G. *Chem. Phys. Lett.* **1993**, *208*, 111−114.
(18) (a) Barone, V.; Cossi, M. *J. Phys. Chem. A* **1998**, *102*, 1995−2001. (b) Cossi, M.; Rega, N.; Scalmani, G.; Barone, V. *J. Comput. Chem.* **2003**, *24*, 669−681.
(19) Zhao, Y.; Truhlar, D. G. *J. Chem. Phys.* **2006**, *125*, No. 194101.
(20) Braga, A. A. C.; Ujaque, G.; Maseras, F. *Organometallics* **2006**, *25*, 3647−3658.
(21) Berke, H. *ChemPhysChem* **2010**, *11*, 1837−1849.
(22) (a) Ito, H.; Saito, T.; Miyahara, T.; Zhong, C.; Sawamura, M. *Organometallics* **2009**, *28*, 4829−4840. (b) Labouille, S.; Escalle-Lewis, A.; Jean, Y.; Mézailles, N.; Le Floch, P. *Chem.—Eur. J.* **2011**, *17*, 2256−2265.
(23) (a) Jee, J. E.; Comas-Vives, A.; Dinoi, C.; Ujaque, G.; van Eldik, R.; Lledós, A.; Poli, R. *Inorg. Chem.* **2007**, *46*, 4103−4113. (b) Fernandes, P. A.; Ramos, M. J. *Chem.—Eur. J.* **2004**, *10*, 257−266. (c) Marx, D.; Tuckerman, M. E.; Hutter, J.; Parrinello, M. *Nature* **1999**, *397*, 601−604. (d) Schmitt, U. W.; Voth, G. A. *J. Chem. Phys.* **1999**, *111*, 9361−9381. (e) Siegbahn, P. E. M. *J. Phys. Chem.* **1996**, *100*, 14672−14680. (f) Tuñón, I.; Silla, E.; Bertrán, J. *J. Phys. Chem.* **1993**, *97*, 5547−5552. (g) Wei, D. Q.; Salahub, D. R. *J. Chem. Phys.* **1994**, *101*, 7633−7642. (h) Comas-Vives, A.; Lledós, A.; Poli, R. *Chem.—Eur. J.* **2010**, *16*, 2147−58. (i) Comas-Vives, A.; Stirling, A.; Lledós, A.; Ujaque, G. *Chem.—Eur. J.* **2010**, *16*, 8738−8747.
(24) Osborn, J. A.; Jardine, F. H.; Young, J. F.; Wilkinson, G. *J. Chem. Soc. A* **1966**, 1711−1732.
(25) Daniel, C.; Koga, N.; Han, J.; Fu, X. Y.; Morokuma, K. *J. Am. Chem. Soc.* **1988**, *110*, 3773−3787.
(26) (a) Haack, K. J.; Hashiguchi, S.; Fujii, A.; Ikariya, T.; Noyori, R. *Angew. Chem., Int. Ed. Engl.* **1997**, *36*, 285−288. (b) Yamakawa, M.; Ito, H.; Noyori, R. *J. Am. Chem. Soc.* **2000**, *122*, 1466−1478.
(27) Comas-Vives, A.; Ujaque, G.; Lledós, A. *Adv. Inorg. Chem.* **2010**, *62*, 231−260.
(28) Noyori, R.; Hashiguchi, S. *Acc. Chem. Res.* **1997**, *30*, 97−102.
(29) Comas-Vives, A.; Ujaque, G.; Lledós, A. *THEOCHEM* **2009**, *903*, 123−132.
(30) (a) Bullock, R. M. *Chem.—Eur. J.* **2004**, *10*, 2366−2374. (b) Bullock, R. M. In *Handbook of Homogeneous Hydrogenation*; de Vries, J. G., Elsevier, C. J., Eds.; Wiley-VCH: Weinheim, Germany, 2007; Vol. *1*, p 153. (c) Guan, H. R.; Iimura, M.; Magee, M. P.; Norton, J. R.; Zhu, G. *J. Am. Chem. Soc.* **2005**, *127*, 7805−7814.
(31) The energy of the transition state for the proton transfer was affected by the presence of an additional solvent (EtOH) molecule. In additional tests we found that incorporating more than two solvent molecules did not significantly modify the relative energy barrier (see the Supporting Information). Thus, unless otherwise stated, two solvent molecules were included in the calculations when the process of proton transfer coming from the solvent was evaluated.
(32) Perez-Temprano, M. H.; Casares, J. A.; Espinet, P. *Chem.—Eur. J.* **2012**, *18*, 1864−1884.
(33) Privalov, T.; Samec, J. S. M.; Bäckvall, J.-E. *Organometallics* **2007**, *26*, 2840−2848.
(34) (a) Schmidbaur, H.; Schier, A. *Chem. Soc. Rev.* **2008**, *37*, 1931−1951. (b) Schmidbaur, H.; Schier, A. *Chem. Soc. Rev.* **2012**, *41*, 370−412.